Cardiac neural crest contributes to cardiomyocytes in amniotes and heart regeneration in zebrafish

Weiyi Tang[1+], Megan L. Martik[1+], Yuwei Li[1] and Marianne E. Bronner[1]*

[1]Division of Biology and Biological Engineering

California Institute of Technology

Pasadena, 1200 E California Blvd, CA 91125, USA

*Correspondence to: mbronner@caltech.edu

[+] These authors contributed equally.

Abstract:

Cardiac neural crest cells contribute to important portions of the cardiovascular system including the aorticopulmonary septum and cardiac ganglion. Using replication incompetent avian retroviruses for precise high-resolution lineage analysis, we uncover a previously undescribed neural crest contribution to cardiomyocytes of the ventricles in *Gallus gallus*, supported by *Wnt1-Cre* lineage analysis in *Mus musculus*. To test the intriguing possibility that neural crest cells contribute to heart repair, we examined *Danio rerio* adult heart regeneration in the neural crest transgenic line, *Tg(-4.9sox10:eGFP)*. Whereas the adult heart has few *sox10+* cells in the apex, *sox10* and other neural crest regulatory network genes are upregulated in the regenerating myocardium after resection. The results suggest that neural crest cells contribute to many cardiovascular structures including cardiomyocytes across vertebrates and to the regenerating heart of teleost fish. Thus, understanding molecular mechanisms that control the normal development of the neural crest into cardiomyocytes and reactivation of the neural crest program upon regeneration may open potential therapeutic approaches to repair heart damage in amniotes.

Introduction

The neural crest is an important stem cell population characterized by its multipotency, migratory behavior, and broad ability to differentiate into derivatives as diverse as elements of the cardiovascular system, craniofacial skeleton, and peripheral nervous system. However, not all neural crest cells are alike, with distinct populations existing along the body axis. One of the most unique neural crest populations is the "cardiac neural crest" that contributes to the outflow septum and smooth muscle of the outflow tract of the heart. Ablation studies in chick embryos show that removal of the cardiac crest results in a broad range of defects, including persistent truncus arteriosus, abnormal myocardium function, and misalignment of the arch arteries [1,2,3]. These defects are highly reminiscent of some of the most common human congenital heart defects. Importantly, other neural crest populations cannot rescue the effects of cardiac neural crest ablation, even when grafted in its place, exemplifying the uniqueness of this population [4].

Classically, quail-chick transplantation experiments have been used to uncover contributions of the cardiac neural crest to the heart, with some more recent attempts using antibody staining of migratory neural crest cells or LacZ retroviral lineage analysis as well as transgenic lines such as *Wnt1-Cre* driven β-galactosidase in mammals [1,5-7]. The results suggest that the cardiac neural crest contributes to smooth muscle cells lining the great arteries, outflow tract septum and valves, mesenchyme that remodels pharyngeal arch arteries, and parasympathetic innervation of the heart, such as the cardiac ganglion. However, inconsistencies remain between different lineage approaches, most of which suffer from high background and low cellular resolution.

To reconcile these differences, here, we use a multi-organismal approach to examine the lineage contributions of cardiac neural crest to the heart. Using a novel retroviral labeling approach in chick and confirmed by *Wnt1-Cre* reporter lines in mouse, we reveal a previously undetected contribution of the amniote cardiac neural crest to the trabecular myocardium of the ventricles, a derivative previously thought to be confined to non-amniotic vertebrates [8-10].

The homologous cardiac neural crest contribution to cardiomyocytes across diverse species raised the intriguing possibility that these cells may contribute to cardiac repair. As the adult zebrafish heart exhibits extensive regenerative capacity, we turned to this model to test whether the neural crest may contribute to heart regeneration[11]. Intriguingly, we show that resected adult zebrafish hearts reactivate many genes of a neural crest gene regulatory program during the regeneration process. Taken together, these results demonstrate an evolutionarily conserved contribution of neural crest cells to cardiomyocytes across vertebrates and a previously unappreciated role during heart regeneration.

Results

Labeling the chick cardiac neural crest using Replication Incompetent Avian retrovirus

To specifically label cardiac neural crest cells prior to their emigration from the neural tube and identify novel progeny of chick cardiac crest, we use a replication-incompetent avian retrovirus (RIA) that indelibly and precisely marks neural crest progenitors for long term lineage analysis at single cell resolution and without the need for tissue grafting. To this end, the post-otic neural tube of the hindbrain adjacent to somites 1-3 was injected at Hamburger and Hamilton (HH) stage 9-10 with high-titer ($1x10^7$ ifu/mL) RIA (Fig1A), which drives expression of nuclear localized *H2B-YFP* under control of a constitutive RSV promoter [12-16]. At this stage in the development, premigratory cardiac neural crest cells are positioned within the dorsal neural tube and about to emigrate. Accordingly, this labeling approach solely marks hindbrain neural tube cells including premigratory cardiac neural crest cells that subsequently delaminate from the dorsal neural tube during a two-hour time window when the virus remains active.

Virally infected embryos were then allowed to develop for 1-9 days post injection, cryo-sectioned, and analyzed using confocal microscopy. One day after injection, whole mount imaging revealed RIA-labeled cells migrating in a stream along pharyngeal arch 3 (Fig 1B,B'), that subsequently accumulated in pharyngeal arches 3, 4 and 6 two days after infection (Fig 1C). Next, we confirmed that all labeled cells in the periphery co-localized with the migratory neural crest marker, HNK-1, demonstrating that the neural crest is the only population labeled with H2B-YFP outside the neural tube, thus verifying specificity of infection (Fig 1D, Fig 1 supplement 1A). With time, labeled cardiac crest cells were observed in numerous and diverse

derivatives, populating the cardiovascular system in a proximal to distal progression (Fig 1E-I, Supplementary file 1a). Consistent with quail-chick chimera, we observed RIA-labeled cells adjacent to and within the walls of pharyngeal arch arteries, in the aorticopulmonary septum, outflow tract, and cardiac cushion. Moreover, we definitively observed YFP-labeled cells in the superior interventricular septum, a site for which the neural crest contribution has been controversial, although ventricular septal defects are common after cardiac neural crest ablation[17]. The cells of the outflow tract septum and pharyngeal arch arteries differentiated into smooth muscle actin (SMA) positive cells on embryonic day (E) 5 (Fig 2A,B).

Importantly, by E3 and onward, virally labeled neural crest cells were observed in the myocardium of both the outflow tract and the ventricles, where they expressed the myocardial markers, Troponin T and Myosin Heavy Chain (Fig 1H, Fig 1 supplement 1B, outflow tract; Fig 2 C,D, Fig 2 supplement 1A,B, ventricles). These neural crest-derived cardiomyocytes were not actively undergoing cell division or programmed cell death (Fig 2E,F), consistent with the stable presence of cells observed over time (Fig 1I, Supplementary file 1a,1b). Supplementary file 1a and 1b present quantification of contributions of virally labeled cells in the chick ventricular myocardium. While previous lineage tracing experiments in zebrafish showed that a stream of neural crest cells integrate into the myocardium of the primitive heart tube to give rise to cardiomyocytes, our results present the first evidence of a homologous neural crest contribution to cardiomyocytes in chick embryos[8-10].

Lineage analysis in the mouse embryo

To test whether the contribution of cardiac neural crest cells to the myocardium was

conserved in mammals, we examined *Wnt1-Cre;ZsGreen*$^{fl/fl}$ transgenic mice in which neural crest cells were labeled with cytoplasmic GFP[18]. Embryos were fixed at E15.5 (similar to E7 in chick). Analogous to the results in chick embryos, we observed a large number of ZsGreen-positive myocardial cells in the outflow tract and ventricles, as confirmed by Troponin T expression (Fig 3A-C). To avoid ectopic expression that has been associated with the *Wnt1-Cre;ZsGreen*$^{fl/fl}$ transgenic line due to endogenous *Wnt1* activation caused by in-frame ATG located upstream of *Wnt1* start codon, we tested an improved Wnt1 line (*Wnt1-Cre2+; R26mTmG* mouse line) without ectopic activation of canonical *Wnt/β-catenin* pathway[19]. The results were similar to those observed with the *Wnt1-Cre;ZsGreen*$^{fl/fl}$ transgenic mice (Fig 3D,E). As in the chick embryos, murine neural crest derived cells were present in the outflow tract, interventricular septum, and myocardium of both ventricles.

The numbers of neural crest-derived cells appear to decrease with distance along the proximal-to-distal axis (Fig3 supplement 1A), such that no neural crest-derived cardiomyocytes were observed in the apex of the heart (Fig3 supplement 1D,E). As in the chick, the numbers of *Wnt1*+ cells remain stable with time, and the cells do not appear to undergo active cell division or apoptosis (Fig3 supplement 1B,B',C,C'). This contribution persists postnatally, as *Wnt1*+ cells are present at postnatal day 2 (Fig3 supplement 1F-H). These results are consistent with previous studies using less specific P0-cre lines and demonstrate that comparable cardiac crest contributions occur in birds and mammals[20, 21]. Quantification of numbers of neural crest lineage labeled cells in the trabeculated myocardium of mice reveals that they represent approximately 17% of the population in the proximal half of the ventricle (Supplementary file 1a).

The lineage contributions of neural crest-derived cells in chick and mouse are remarkably similar to those previously shown in zebrafish[8-10]. In all three species, neural crest cells

contribute to cardiomyocytes of the trabecular myocardium. This homologous lineage contribution in both amniotes and anamniotes raised the intriguing possibility that neural crest cells may represent a cell population that could contribute to heart repair in adults.

Reactivation of neural crest gene regulatory genes during adult zebrafish heart regeneration

In adult birds and mammals, cardiac injury leads to scarring with little regeneration, whereas heart regeneration is common in amphibians and fish [22]. For example, adult zebrafish have the capacity to regenerate their hearts after removal of up to 20% of the ventricle. This has been shown to occur by dedifferentiation and proliferation of pre-existing cardiomyocytes[11,23]. Given that cardiac neural crest cells give rise to a portion of zebrafish cardiomyocytes during development[8-10] similar to those we report here in chick and mouse, we next asked whether the progeny of these cells might have the ability to contribute to heart regeneration in adult zebrafish.

To address this possibility, we first turned to a transgenic line expressing GFP under the control of a *sox10* promoter, *Tg*(-4.9*sox10:eGFP),* that labels all embryonic migratory neural crest lineages to address whether neural crest-derived cardiomyocytes reactivated their developmental program upon injury[24].

While *sox10* is expressed in migrating zebrafish cardiac neural crest cells, it is down-regulated in the embryo shortly after these cells reach the heart [10]. We confirmed this in adult hearts, finding that very few cells within the apex of the adult myocardium of control adult fish expressed *sox10* one month post-sham injury, in which the body cavity was opened but no resection was made (Fig 4A, Supplementary file 1c, n=3). However, after surgical removal of

~20% of the ventricular apex, cells in the heart reactivated the *sox10* promotor sequence and began to re-express GFP in cardiomyocytes of the trabeculated myocardium near the injured site by 7 days post resection (dpa) (Fig 4A; n=6). GFP expression was not limited to the regenerating tissue but was also observed in the uninjured part of the ventricle. By 21dpa, the hearts had undergone vast regeneration and morphologically were nearly indistinguishable from controls (Fig 4A; n=6). Interestingly, consistent with our prediction, the regenerating apex was comprised of more *sox10+* positive cells (Fig 4A,B, Supplemental file 1C), suggesting that these cells had proliferated and redeployed a neural crest gene regulatory program during the heart regeneration process.

To test if *sox10* and other bona fide neural crest markers such as *tfap2a,* were upregulated endogenously, we performed *in situ* hybridization on paraffin sections of regenerating and uninjured ventricles. The results reveal upregulation of expression of *sox10* and *tfap2a* transcripts after injury, whereas they were mostly absent from uninjured ventricles (Fig 4B,C). Furthermore, we observed co-localization of *sox10* transcripts with a *Tg(sox10:GAL4-UAS-Cre;ubi-Switch),* which permanently labels all sox10-derived lineages with mCherry (Fig4-supplement 1, n=2). The *Tg(sox10:GAL4-UAS-Cre;ubi-Switch)* is a double transgenic line for the *sox10:GAL4-UAS-Cre* transgene and the *ubi:Switch* reporter in which the *sox10* promoter drives expression of Cre recombinase. Upon activation of *sox10* expression in neural crest cells, eGFP is excised and so cells of the *sox10* lineage are permanently labeled with mCherry [10]. All cells expressing *sox10+* transcripts also had mCherry, though not all mCherry positive cells were *sox10+* at the 7 day time point (Fig4-supplement 1, insets 1 and 2). Our results are consistent with recent findings from Abdul-Wajid and colleagues, who observed that ablation of the embryonic neural crest yields few or no sox10+ cells in the adult heart and results in severe heart

188 defects [25]. This suggests there are no subsequent post-embryonic neural crest additions to the
189 heart and that the population we observe re-expressing neural crest genes are embryonic-derived
190 neural crest progeny.

191 These results raise the intriguing possibility that the neural crest developmental gene
192 regulatory network was being redeployed in neural crest-derived cells of the heart during
193 regeneration. To test this, we performed transcriptional profiling of *sox10:mRFP+* cells in the
194 regenerating zebrafish hearts at 21dpa. To this end, we dissected and dissociated injured
195 ventricles (n=12 per replicate) into single cell suspensions and performed FAC-sorting of
196 *sox10:mRFP+* cells (Fig4-supplement 2A). The results were compared with mRFP negative
197 cardiac cells from the same injured, isolated ventricles. This led to the identification of 1093
198 genes that are significantly enriched (p-adj<0.05, LFC>1) in regenerating *sox10+* cells compared
199 to *sox10-* cells of the same injured ventricles (Fig4D, Fig4-supplement 2). We then compared the
200 differentially expressed genes of isolated 21dpa sox10+ cells to: 1) our recently published chick
201 developmental cardiac neural crest gene regulatory program; 2) known zebrafish neural crest
202 genes, and 3) core neural crest gene regulatory network genes expressed at all axial levels[26-28].
203 The results revealed upregulation of many genes of the embryonic neural crest gene regulatory
204 network at the time of regeneration (Fig4D, 4E).

205 Interestingly, numerous genes known to be responsible for cardiomyocyte proliferation
206 also are expressed in *sox10+* cells upon heart injury (Fig4-supplement 2E)[22]. The co-expression
207 of these genes as well as an upregulation of a cell proliferation gene signature suggests a role for
208 sox10-derived cells in cardiomyocyte proliferation during regeneration (Fig4-supplement 2C).
209 Furthermore, these results suggest that the population of proliferating cardiomyocytes in the

regenerating heart is heterogeneous and comprised of both neural crest- and mesoderm-derived cardiomyocytes[22,29-31].

Discussion

While much attention has been paid to the molecular signals that promote myocardial dedifferentiation and proliferation during regeneration, far less is known about the cell lineages that contribute to the regeneration process. Based on our observation on the lineage relationship between cardiac neural crest cells and cardiomyocytes during development, we propose that neural crest-derived cells (progenitors and/or pre-existing cardiomyocytes) may represent a key population that proliferates and differentiates into new cardiomyocytes after injury.

Our cell lineage labeling results provide direct evidence for a neural crest contribution to the undamaged myocardium of the amniote heart. Furthermore, consistent with previous lineage tracing experiments in zebrafish [10,31], where a proportion of cardiac crest derived-cells were located in the trabeculated myocardium in adult fish, we show that after injury, there is activation of numerous neural crest gene regulatory transcription factors and other neural crest genes during regeneration (Fig 4). While the underlying gene regulatory network of neural crest cells is responsible for formation of cardiomyocytes during normal development, we speculate that it also does so in a similar manner upon injury by redeploying *sox10* and other neural crest gene regulatory network genes. The finding that *sox10*-derived cells are primarily in the proximal trabecular myocardium of the zebrafish heart suggests that these cells must be migrating into to the wound site after injury. Of course, we cannot rule out the possibility that the cells that

reactivate *sox10* and the neural crest program may come from another adult lineage. But in the adult, their molecular signature strongly correlates with that of embryonic neural crest cells (Fig4D, 4E). Whereas our data clearly show that the sox10+ cells contribute to cardiomyocytes (Fig4A), whether they also might contribute to other lineages (e.g. hematopoietic cells) within the regenerated tissue remains to be explored.

Why was the contribution of neural crest cells to cardiomyocytes in amniotes previously missed? Interspecific quail-chick chimera are generated via transplantation of donor tissue into the host, which requires time to heal[1]. If the neural crest cells that migrate to the ventricles are the earliest migrating cells, this population may have been delayed after grafting due to wound healing and hence unable to migrate as far. Alternatively, the labeled cells may have been missed since it can be challenging to identify a small population of dispersed quail cells amongst many more numerous chick cells. Furthermore, cell behavior might be altered when transplanted quail cells are introduced into a chick environment. Our retroviral lineage labeling circumvents these issues by indelibly labeling an endogenous neural crest population without the need for grafting. Moreover, the labeled cells are easily detectable due to their fluorescent readout. For lineage labeling in mice, there were hints in the literature regarding a possible neural crest contribution to cardiomyocytes. However, the experiments were either indirect or used lineage tracing techniques that were not specific to the neural crest. For example, Tomita et al. showed that cells isolated from "cardiospheres" can behave like neural crest cells when injected into chick embryos[20]. In addition, lineage analysis in mouse using a P0-cre line revealed EGFP-positive cells in the myocardium that gather at the ischemic border upon injury[20]. However, P0 is not a neural crest specific marker, making these results inconclusive at the time. In contrast, Wnt1 is the "gold standard" for neural crest labeling and the improved Wnt1 line (*Wnt1-Cre2+;*

R26mTmG) corrects possible ectopic expression problematic in the original *Wnt1-Cre;ZsGreen line*[7,18,19].

In chick and mouse, neural crest-derived cells comprise a significant portion (~17%) of the trabeculated myocardium in the proximal part of both ventricles. Interestingly, this percentage is similar to what has been reported in zebrafish[10,25]. In amniotes, we find that the density of the cells decreases along the proximal-distal axis and appears to be stable through time (Fig1I, Supplemental file 1A, B). The presence of neural crest-derived cardiomyocytes across vertebrates and the redeployment of a *sox10+* cell population in zebrafish heart regeneration suggest that the neural crest-derived myocardium might also play a role in heart regeneration in neonatal mice, which requires further testing.

In summary, the present results show, for the first time, the common ability of cardiac neural crest cells across diverse vertebrates to contribute to heart muscle. Moreover, these cells appear to be critical for cardiac regeneration in zebrafish. If the results extrapolate to other species, the mechanisms that control the normal development of the neural crest into cardiomyocytes may be harnessed to stimulate these cells to proliferate and regenerate new cardiomyocytes, thus offering potential therapeutic approaches to repair heart damage in mammals including humans.

Materials and Methods:

Key Resources Table

Reagent type (species) or resource	Designation	Source or reference	Identifiers	Additional information
Genetic reagent (*Mus musculus*)	*Wnt1-Cre; ZsGreen$^{fl/fl}$*	PMID:10725243	Jackson Laboratories, Stock# 003829	Drs. Xia Han and Yang Chai at University of Southern California, Center for Craniofacial Molecular Biology
Genetic reagent (*Mus musculus*)	*Wnt1-Cre2+((129S4-Tg(Wnt1-cre)1Sor/J));R26mTmG*	PMID: 23648512	Jackson Laboratory, Stock# 22137	Dr. Jeffrey Bush at University of California, San Francisco
Genetic reagent (*Danio rerio*)	*Tg(-4.9sox10:eGFP)*	PMID: 17065232	ZFIN ID: ZDB-TGCONSTRCT-070117-69	
Genetic reagent (*Danio rerio*)	Tg(sox10:GAL4-UAS-Cre;ubi-Switch)	PMID: 26086691		Drs. Ann M. Cavanaugh and Jau-Nian Chen at Department of Molecular, Cell and Developmental biology, University of California, Los Angeles
Genetic reagent (*Danio rerio*)	*Tg(sox10:mRFP)*	PMID: 18176560	ZFIN ID: ZDB-TGCONSTRCT-080321-2	
Cell line	UMNSAH/DF-1	ATCC	#CRL-12203, Lot	

(*Galllus gallus* DF1)	fibroblast spontaneously transformed		number 62712171; RRID:CVCL_0570	
Recombinant DNA reagent	RES-H2B-YFP-DD	Addgene	RRID:Addgene_96893	
antibody	Mouse monoclonal anti-bovine Troponin T, IgG2a (CT3)	DSHB	RRID:AB_528495	Dilution (1:10)
antibody	Mouse monoclonal anti-chicken Myosin Heavy Chain, IgG1 kappa light chain (ALD58)	DSHB	RRID:AB_528361	Dilution (1:10)
antibody	Mouse monoclonal anti-chicken Myosin Heavy Chain, IgG1 kappa light chain (F59)	DSHB	RRID:AB_528373	Dilution (1:10)
antibody	Mouse monoclonal anti-NH2 terminal synthetic decapeptide of alpha smooth muscle actin, IgG2a	Sigma	# A5228	Dilution (1:500)
antibody	Mouse monoclonal anti-human phospho-histone H3, IgG1	Abcam	#ab14955	Dilution (1:500)
antibody	Rabbit polyclonal anti-human Caspase 3, IgG	R&D systems	#AF835	Dilution (1:500)
antibody	Goat polyclonal anti -GFP, IgG	Abcam	#ab6673	Dilution (1:500)
antibody	Goat polyclonal anti-mouse IgG2a Alexa-568	Molecular Probes	RRID:AB_2535773	Dilution (1:1000)
antibody	Goat polyclonal anti-mouse IgG1 Alexa-568	Molecular Probes	RRID:AB_2535766	Dilution (1:1000)
antibody	Goat polyclonal anti-rabbit IgG Alexa-568	Molecular Probes	RRID:AB_2534121	Dilution (1:1000)
antibody	Donkey polyclonal anti-goat IgG Alexa-488	Molecular Probes	RRID:AB_2534102	Dilution (1:1000)
Software, algorithm	Image processing software FIJI	https://imagej.net/Fiji		
Software,	R v3.6.1	https://www.r-		

algorithm		project.org/		
Software, algorithm	DESeq2	PMID: 25516281	RRID:SCR_015687	
Software, algorithm	Bowtie2	PMID: 22388286	RRID:SCR_005476	
Software, algorithm	featureCounts (Subread)	PMID: 24227677	RRID:SCR_009803	
Other	Accumax	Innovative Cell Technologies, Inc	#AM105	
Commercial assay or kit	SMART-seq Ultra Low Input RNA Kit V4	Takara Clontech	#634891	

Cell culture and retrovirus preparation

Using a standard transfection protocol, chick DF1 cells (ATCC, Manassas, VA; #CRL-12203, Lot number 62712171, RRID:CVCL_0570, Certificate of Analysis with negative mycoplasma testing at the ATCC website) were transfected with RIA-H2B-YFP plasmid (RRID:Addgene_96893) and ENV-A plasmid in 15 cm culture dishes. Cell culture medium was collected 24 hours post-transfection, and twice per day for four days, then centrifuged at 26,000 rpm for 1.5 hr. The supernatant was dried with aspiration, and the pellet was dissolved in 20-30 µl of DMEM to a final titer of 1×10^7 ifu/mL. Viral aliquots were stored in -80°C until the time of injection.

Chick embryo processing and viral injection

Viral stock was diluted 1:2 with Ringer's solution (0.9% NaCl, 0.042%KCl, 0.016%$CaCl_2 \bullet 2H_2O$ wt/vol, pH7.0) to generate the working solution, which was mixed with 0.3µl of 2% food dye (Spectral Colors, Food Blue 002, C.A.S# 3844-45-9) as indicator. The lumen of the neural tube adjacent to the middle of the otic vesicle to the level of somite 3 was injected with 0.2µl of working in HH8-10 chicken embryos. Embryos were sealed with surgical tap and incubated at

37°C for 1-10 days, harvested at HH14 (n=5), HH18 (n=5), HH21 (n=4), HH25 (n=4), HH28 (n=4), HH32 (n=4) and E10 (n=4). At the time of harvesting, chick embryos were dissected, fixed in 4%PFA in PBS for 30 mins at 4°C, then embedded in gelatin and sectioned (*Microm* HM550 cryostat).

Wnt1-Cre mouse and tissue preparation

The *Wnt1-Cre; ZsGreen*$^{fl/fl}$ mice described in Chai *et al*., 2000 (gift from Drs. Xia Han and Yang Chai at University of Southern California, Center for Craniofacial Molecular Biology) were harvested and fixed at E15.5 (n=8) and P2 (n=2). The hearts were dissected, fixed in 4%PFA in PBS for 30mins at 4°C. E15.5 *Wnt1-Cre2+; R26mTmG* mice (Lewis *et al*.,2013) (129S4-Tg(Wnt1-cre)1Sor/J, gift from Dr. Jeffrey Bush at University of California, San Francisco, n=3) were fixed with 4% PFA overnight before dissection. The hearts were embedded in gelatin, and sectioned.

Quantification of neural crest contributions to the ventricular myocardium and regeneration

To quantify RIA-labeled cells in chick embryos, three consecutive sections of the same axial level were imaged per embryo. The number of YFP-positive cells was averaged to account for variability due to sampling. n=4-6 embryos were analyzed at each stage as biological replicates. The results are presented as presence or absence of virally labelled cardiac neural crest derivatives at different anatomical locations in Fig. 1I and supplementary file1a, 1b. To quantify Wnt1-Zsgreen+ cells in E15.5 mouse heart, three consecutive sections of the same axial level were imaged per embryo (n=4). Automated particle analysis was conducted with FIJI program to estimate the total number of Zsgreen+ cells in the image. For the percentage of neural crest-derived cells in the ventricle, the same procedure was performed with the DAPI channel which represents total cell population. % Zsgreen/DAPI was calculated, and averaged to the result

315 presented in the text of supplementary file 1a. Same analysis was conducted to estimate the
316 number of *sox10:eGFP*+ cells in 7dpa (n=3), 21dpa (n=3) and sham operated (n=3) hearts in an
317 area of $2x10^5 \mu m^2$ at the apex. One section per heart at the middle of the apex was quantified and
318 presented in supplementary file 1c.

319 Zebrafish cardiac injury and tissue collection

320 Adult zebrafish heart resection was conducted with the *Tg(-4.9sox10:eGFP)* or *Tg(sox10:mRFP)*
321 line, according to published protocols (Poss *et al*., 2002). Resected and sham operated fish hearts
322 (n=24) were collected at 7 days post injury (dpi) (n=18), and 21 dpi (n=53) at which time the fish
323 were euthanized and the hearts were removed for further analysis. The hearts were fixed in
324 4%PFA in PBS for overnight at 4°C prior to processing for staining. Adult zebrafish were
325 maintained in the Beckman Institute Zebrafish Facility at Caltech, and all animal and embryo
326 work were completed in compliance with California Institute of Technology Institutional Animal
327 Care and Use Committee (IACUC) protocol 1764.

328 Immunohistochemistry and image analysis

329 After cryosectioning, slides were incubated in 1xPBS at 42°C to remove gelatin. 0.3% vol/vol
330 Triton-X100in 1xPBS was used to permeabilize the tissue. Sections were incubated with primary
331 antibody underneath a parafilm layer at 4°C overnight (primary antibody dilutions: 1:10
332 Troponin T CT3, DSHB (RRID:AB_528495); 1:10 Myosin Heavy Chain ALD58, DSHB
333 (RRID:AB_528361); 1:10 Myosin Heavy Chain F59, DSHB (RRID:AB_528373); 1:500 Mouse
334 anti-smooth muscle actin, Sigma-Cat# A5228-200uG; 1:500 Mouse anti phospho-histone H3,
335 Abcam-ab14955; 1:500 rabbit anti caspase-3,R&D Systems # AF835; 1:500 goat anti GFP,
336 Abcam Cat#ab6673, all in blocking reagent 1xPBS with: 5% vol/vol normal donkey serum, 0.3%
337 vol/vol Triton-X100). Subsequently, sections were washed for 3 times with 1xPBS, incubated

with secondary antibody for 40 mins at room temperature and counterstained with DAPI. Secondary antibodies include: Goat anti-mouse IgG2a Alexa-568 (RRID:AB_2535773), Goat anti-mouse IgG1 Alexa-568(RRID:AB_2535766), Goat anti-rabbit IgG Alexa-568(RRID:AB_2534121), Donkey anti-goat IgG Alexa-488(RRID:AB_2534102); 1:1000, Molecular Probes. Zeiss AxioImager.M2 with Apotome.2 and Zeiss LSM 800 confocal microscope were utilized for imaging. Images were cropped, rotated, and intensity was linearly adjusted for visualization.

In situ hybridization of adult zebrafish hearts

After fixation, hearts were embedded in paraffin and sections were prepared at 10µm thickness on a Zeiss microtome. After paraffin removal with histosol, sections were hybridized with 1ng/µl anti-sense digoxygenin-labelled probes overnight at 70°C in a humidifying chamber. After hybridization, sections were washed with 50% formamide/50% 1X SSCT buffer followed by washes with MABT and a blocking step in 1% Roche blocking reagent. Sections were then incubated overnight at room temperature with a 1:2000 dilution of anti-DIG-Alkaline Phosphatase antibody (Roche). After several washes with MABT, chromogenic color was developed using NBT/BCIP precipitation (Roche).

Transcriptome analysis of regenerating neural crest cells

For each replicate (n=2), regenerating ventricles (n=12) were isolated at 21 days post injury and dissociated into a single cell suspension using a pestle-A tissue homogenizer followed by incubation in Accumax (Innovative Cell Technologies, Inc.) at 30°C. *sox10*-mRFP-positive and *sox10*-mRFP-negative cells were collected by FAC-sorting on a BD Biosciences FACSAriaFusion Cell Sorter. cDNA from mRFP-positive and negative cells was prepared using SMART-seq Ultra Low Input RNA Kit V4 (Takara) according to the manufacturer's protocol.

Sequencing libraries were built according to Illumina Standard Protocols and sequenced using an Illumina HiSeq2500 sequencer at the Millard and Muriel Jacobs Genetics and Genomics Laboratory (California Institute of Technology, Pasadena, CA). 50 million, 50bp, single-ended reads from two biological replicates were mapped to the zebrafish genome (GRCz10) using Bowtie2 [33]. Transcript counts were calculated using featureCounts (Subread) and differential gene expression analysis was performed using DESeq2 [34,35]. Protein classification analysis was performed using PANTHER [36]. Heatmaps of normalized counts were generated using Heatmap2. Databases have been deposited to NCBI (BioProject # PRJNA526570).

Acknowledgments:

We would like to thank Drs. Xia Han and Yang Chai at University of Southern California, Center for Craniofacial Molecular Biology for being extremely supportive and kindly providing *Wnt1-Cre; ZsGreen*$^{fl/fl}$ cardiac tissue. Many thanks to Dr. Jeffrey Bush at University of California, San Francisco who generously sent us *Wnt1-Cre2+; R26mTmG* mouse embryos. We appreciate the help from Drs. Ann M. Cavanaugh and Jau-Nian Chen at Department of Molecular, Cell and Developmental biology, University of California, Los Angeles in sharing *Tg (NC: mCherry)* transgenic fish line for *Sox10:GAL4-UAS-Cre;ubi:Switch*. We would also like to acknowledge the Caltech Millard and Muriel Jacobs Genetics and Genomics Laboratory, in particular, Igor Antoshechkin for sequencing of our RNAseq libraries. We thank Rochelle Diamond and Diana Perez of the the Caltech Flow Cytometry Cell Sorting Facility for cell sorting assistance. We thank David Mayorga and Ryan Fraser of the Beckman Institute Zebrafish Facility for help with zebrafish husbandry and Joanne Tan-Cabugo and Constanza Gonzalez for technical assistance, and Beckman Institute Biological Imaging Facility for equipment. **Funding:**

This work is supported by NIHR01DE027568 and NIHRO1HL14058 to MEB and a Helen Hay Whitney Post-doctoral Fellowship to MLM.

Competing interests: The authors declare no competing financial interests. Correspondence and request for materials should be addressed to mbronner@caltech.edu.

List of figures and figure supplements:

Figure 1

Figure 1-figure supplement 1

Figure 2

Figure 2-figure supplement 1

Figure 3

Figure 3-figure supplement 1

Figure 4

Figure 4-figure supplement 1

Figure 4-figure supplement 2

Supplementary file:

Supplementary file 1a, 1b, 1c

Figure legends:

Figure 1: Retrovirally mediated fate mapping of cardiac neural crest reveals novel derivatives. (A) Schematic diagram of the approach: Replication Incompetent Avian (RIA)

retrovirus encoding nuclear H2B-YFP was injected into the lumen of the hindbrain from which cardiac neural crest arises. (B) One day post-infection (HH14), whole mount image (lateral view) showing virally labelled progeny (green) in the cardiac migration stream en route to pharyngeal arch 3. (B') Brightfield image to show anatomical information. A, anterior; P, posterior; D, dorsal; V, ventral. (C) Two days post-infection (HH18), virally labelled cardiac crest has populated pharyngeal arches 3, 4 and 6, highlighted with dashed line. (D) Transverse section showing that labelled cardiac crest expresses neural crest marker HNK-1 (red). D, dorsal; V, ventral; L, left; R, right. (E) Low magnification transverse section of an E6 embryo (DAPI, blue). Dashed boxes show relative positions of cardiac crest-derived populations. (F-H) High magnification image of selected regions in E: pharyngeal arch arteries (F); aorticopulmonary septum (G); Neural crest derivatives located in the outflow tract express Troponin T (magenta), a myocardium marker (H, H'). (I) Temporal map of the establishment of distinct cardiac neural crest derivatives. Labelled cells initially are in the migration stream, cranial nerve IX (CN-IX) and mesenchyme around pharyngeal arch arteries (PAA). Subsequently, they populate the aorticopulmonary septum (APS), myocardium (MYO) and interventricular septum (IVS). Separate channels are displayed in supplement 1. Light blue indicates known neural crest derivatives. Dark blue reflects newly discovered neural crest derivatives.

Scale bars: B, C, E 400μm; D, F, G, H 100μm.

Figure 1- figure supplement 1: Separate channels for retroviral lineage analysis and immunohistochemistry. (A) Separate channels of Figure 1D. All H2B-YFP labelled cells that migrate out of the neural tube are HNK1-positive cardiac neural crest cells (H2B-YFP, green; HNK1, red; DAPI, blue). (B) Separate channels of Figure 1H. H2B-YFP labelled cardiac

neural crest is present in myocardium of the outflow tract (H2B-YFP, green; Troponin T, magenta; DAPI, blue).

Figure 2: Cardiac crest-derived cells differentiate into smooth muscle and cardiomyocytes in avian embryos. (A, B) Retrovirally labelled cardiac crest cells (H2B-YFP, green) that migrate into the outflow tract (A, OFT) and pharyngeal arch arteries (B) express smooth muscle actin (SMA, magenta) marker. (C, D) Labeled cardiac crest cells that enter the ventricle express myocardial marker Troponin T (magenta) (C), and myocardial terminal differentiation marker Myosin Heavy Chain (MHC, magenta) (D) enclosed in dashed line. (E, F) Neural crest-derived cardiomyocytes are not actively dividing or undergoing apoptosis, as demonstrated by phosphohistone H3 staining (PH3, magenta) (E) and Caspase 3 staining (magenta) (F). Transverse view of HH28 embryos. Separate channels are displayed in supplement 1. Scale bars: 100μm.

Figure 2-figure supplement 1: Separate channels for retroviral lineage analysis and immunohistochemistry. (A) Separate channels of Figure 2C. H2B-YFP virus labelled cardiac neural crest is present in myocardium of the ventricle and expresses cardiomyocyte marker Troponin T (H2B-YFP, green; Troponin T, magenta; DAPI, blue; enclosed in dashed line). (B) Separate channels of Figure 2D. H2B-YFP virus labelled cardiac neural crest is present in myocardium of the ventricle and expresses cardiomyocyte terminal differentiation marker myosin heavy chain (MHC) (H2B-YFP, green; MHC, magenta; DAPI, blue; enclosed in dashed line).

Figure 3: *Wnt1-Cre* fate mapping in mice confirms the presence of cardiac crest-derived myocardium. (A) Low magnification image to show the relative anatomical positions of a mouse heart at E15.5 (sagittal view, DAPI-blue). (B, C) In *Wnt1-Cre; ZsGreen*$^{fl/fl}$ mice, neural crest-derived cells (green, *Wnt1-Cre* driven ZsGreen expression is abbreviated as Wnt1-ZsGreen, enclosed in dashed line) were observed in myocardium (Troponin T, grey) of the outflow tract (B), and ventricle (VENT) (C, C'': separate channels of inset C'). (D, E) Similar results were obtained from *Wnt1-Cre2+; R26mTmG* mice (*Wnt1-Cre2+* driven replacement of membrane localized tdTomato (mT) by EGFP (mG) (abbreviated as Wnt1-mtmg), where cardiac crest-derived cells (green, enclosed in dashed line) were present in myocardium of the outflow tract (D) and ventricle (Troponin T, grey) (E, E'': separate channels of inset E'). Transverse view. Spatial-temporal information and antibody staining are displayed in supplement 1.
Scale bars: A 400μm; B-E 100μm; C', E' 10μm.

Figure 3-figure supplement 1: Spatial-temporal distribution of neural crest-derived cardiomyocytes in *Wnt1-Cre* mouse. (A) In E15.5 *Wnt1-Cre; Zsgreen*$^{fl/fl}$ mouse heart, cardiac neural crest progenies were distributed in the outflow tract, valves and myocardium of both ventricles. Density of Zsgreen+ cells decreased along the proximal-to-distal axis, thus no cell contributed to the apex (Wnt1-Zsgreen, green; Troponin T, red; DAPI, blue). (B) Proliferation marker PH3 did not selectively colocalize with Zsgreen+ cells (PH3, magenta; B', separate channels for colocalization). (C) Apoptosis marker Caspase3 was not selectively expressed in Zsgreen+ cells (Caspase 3, magenta; C', separate channels for colocalization). (D) Cardiac neural crest did not contribute to apical myocardium in *Wnt1-Cre; Zsgreen*$^{fl/fl}$ *mouse* (Wnt1-Zsgreen, green; Troponin T, red; DAPI, blue), or (E) *Wnt1-Cre; R26mtmg* mouse (Wnt1-

membrane GFP, green; membrane Tomato, red; DAPI, blue). (F-H) On postnatal day 2, cardiac neural crest progenies in Wnt1-ZsGreen mouse persisted in the myocardium of the ventricle (F) (separate channels in F'), outflow tract (G), but not the apex (H) (Wnt1-Zsgreen, green; Troponin T, red; DAPI, blue), similar to what was observed in E15.5 hearts.
Scale bars: A 400μm; B, C, F, G 100μm; D, E, H 160μm.

Figure 4: Cardiac neural crest contributes to heart regeneration in zebrafish. (A) In sham-operated adult zebrafish hearts from a transgenic line expressing GFP under the control of a sox10 promoter, very few cells expressed *Tg(-4.9sox10:eGFP)* (green) (n=3). 7 days-post amputation (dpa), the *sox10* promoter was reactivated as shown by GFP+ cells in the trabeculated myocardium near the site of injury (*Tg(-4.9sox10:eGFP),* green) (n=6). 21dpa, when the resected apex regenerated, more GFP+ cells were observed in sagittal sections within and surrounding the site of injury (n=6). Sections in A are counterstained with DAPI in blue and Myosin Heavy Chain in red. (B) Endogenous *sox10* mRNA expression was observed by paraffin section *in situ* hybridization in uninjured, 7dpa, and 21dpa hearts. Arrows denote cells with *sox10* expression. From these results, we conclude that *sox10* is reactivated after injury. (C) Along with *sox10,* expression of neural crest marker, *tfap2a,* was also enriched after injury. Arrows label areas of expression in the myocardium. (D) Differential gene expression analysis of FACS-sorted *Tg(sox10:mRFP)*+ and FACS-sorted *Tg(sox10:mRFP)*- transcriptomes show n=1093 genes are enriched at 21dpa in the *sox10*+ cells compared to the rest of the ventricular tissue (n=12 ventricles per replicate). Zebrafish neural crest genes as determined by GO analysis are highlighted on the volcano plot. (E) Upregulation of neural crest gene regulatory network genes was also observed from our differential expression analysis (**$p<0.05$, ***$p<0.001$). Co-

localization of *sox10* mRNA expression with Tg(sox10:GAL4-UAS-Cre;ubi:Switch)+ neural crest-derived cardiomyocytes is presented in supplement 1; schematic diagram of experimental design for obtaining the regenerating neural crest transcriptome and further analysis of gene enrichments is presented in supplement 2.

Scale bars: 100μm

Figure 4-figure supplement 1: Co-localization of sox10 mRNA expression with Tg(sox10:GAL4-UAS-Cre;ubi:Switch)+ neural crest-derived cardiomyocytes. *sox10* transcript in adult zebrafish regenerating hearts (7dpa are reactivated in cells labeled by neural crest lineage transgenic line, *Tg(sox10:GAL4-UAS-Cre;ubi:Switch)* that permanently marks all neural crest-derived cells with mCherry (red). mCherry+ neural crest-derived cardiomyocytes were located in both the compacted and trabeculated layers of the ventricle. While not all neural crest-derived cells expressed *sox10* (1), *sox10* transcripts were only present in mCherry positive cells (2).

Scale bar: 100μm.

Figure 4-figure supplement 2: Analysis of regenerating neural crest transcriptome. (A) Experimental design for the transcriptome analysis of regenerating neural crest cells. 1. Hearts were resected and ventricles were collected and dissociated at 21dpa, 2. mRFP+ and mRFP- cells were collected by FAC-sorting (FACS plot shows gating of populations). (B) Panther classification of proteins encoded by upregulated genes in the *sox10+* cells. (C) Bar plot showing enriched mitotic cell cycle genes. (D) Bar plot showing enriched transcription factors. (E) Heatmap of normalized counts for known genes implicated in heart regeneration.

Supplementary File 1

a, b: Quantification of cardiac neural crest contribution to the heart in chick and mouse.

Table presents virally labelled cardiac neural crest derivatives at MNC (migratory neural crest), CN-IX (cranial nerve nine), PAA (pharyngeal arch arteries), APS (aorticopulmonary septum), MYO (myocardium of ventricle) and IVS (interventricular septum) at day 1-6 and day 10 post injection in chick. The bottom part presents number of Wnt1+ cells in E15.5 *Wnt1-Cre* mouse. Percentage in parentheses represents the proportion of the population among all NC-derived cells in cardiovascular structure (including MYO, APS, and IVS). % Neural crest contribution to ventricle, the proportion of Wnt1+ cells (including MYO and IVS) among all cells in the ventricle is about 16.8%. Supplementary File 1b shows the raw data of each embryo from which data in Supplementary File 1a was generated.

c: Quantification of *sox10:eGFP+* cells in the apex during zebrafish heart regeneration.

Average number of *Sox10-eGFP+* cells per $2x10^5$ μm^2 in one section through the middle of the apex of 7dpa (n=3) and 21 dpa (n=3) hearts after resection. Standard deviation is presented in parentheses next to the cell number. GFP expression was negligible in sham operated hearts (n=3) at the same time points.

References:

1. Kirby M, Gale T, Stewart D. Neural crest cells contribute to normal aorticopulmonary septation. *Science*. 1983;220(4601):1059-1061. doi:10.1126/science.6844926.

2. Waldo K, Zdanowicz M, Burch J, et al. A novel role for cardiac neural crest in heart development. *J Clin Invest*. 1999;103(11):1499-1507. doi:10.1172/JCI6501.

3. Bockman DE, Redmond ME, Waldo K, Davis H, Kirby ML. Effect of neural crest ablation on development of the heart and arch arteries in the chick. *Am J Anat*. 1987;180(4):332-341. doi:10.1002/aja.1001800403.

4. Kirby ML. Plasticity and predetermination of mesencephalic and trunk neural crest transplanted into the region of the cardiac neural crest. *Dev Biol*. 1989;134(2):402-412.

5. Kuratani SC, Kirby ML. Initial migration and distribution of the cardiac neural crest in the avian embryo: an introduction to the concept of the circumpharyngeal crest. *Am J Anat*. 1991;191(3):215-227. doi:10.1002/aja.1001910302.

6. Boot MJ, Gittenberger-De Groot AC, Van Iperen L, Hierck BP, Poelmann RE. Spatiotemporally separated cardiac neural crest subpopulations that target the outflow tract septum and pharyngeal arch arteries. *Anat Rec A Discov Mol Cell Evol Biol*. 2003;275(1):1009-1018. doi:10.1002/ar.a.10099.

7. Jiang X, Rowitch DH, Soriano P, McMahon AP, Sucov HM. Fate of the mammalian cardiac neural crest. *Development*. 2000;127(8):1607-1616.

8. Sato M, Yost HJ. Cardiac neural crest contributes to cardiomyogenesis in zebrafish. *Dev Biol*. 2003;257(1):127-139. doi:10.1016/S0012-1606(03)00037-X.

9. Li Y-X, Zdanowicz M, Young L, Kumiski D, Leatherbury L, Kirby ML. Cardiac neural crest in zebrafish embryos contributes to myocardial cell lineage and early heart function. *Dev Dyn*. 2003;226(3):540-550. doi:10.1002/dvdy.10264.

10. Cavanaugh AM, Huang J, Chen J-N. Two developmentally distinct populations of neural crest cells contribute to the zebrafish heart. *Dev Biol*. 2015;404(2):103-112. doi:10.1016/j.ydbio.2015.06.002.

11. Poss KD, Wilson LG, Keating MT. Heart regeneration in zebrafish. *Science*. 2002;298(5601):2188-2190. doi:10.1126/science.1077857.

12. Li Y, Li A, Junge J, Bronner M. Planar cell polarity signaling coordinates oriented cell division and cell rearrangement in clonally expanding growth plate cartilage. *Elife*. 2017;6. doi:10.7554/eLife.23279.

13. Tang W, Li Y, Gandhi S, Bronner ME. Multiplex clonal analysis in the chick embryo using retrovirally-mediated combinatorial labeling. *Dev Biol*. 2019;450(1):1-8. doi:10.1016/j.ydbio.2019.03.007.

14. Fields-Berry SC, Halliday AL, Cepko CL. A recombinant retrovirus encoding alkaline phosphatase confirms clonal boundary assignment in lineage analysis of murine retina. *PNAS*. 1992;89(2):693-697. doi:10.1073/pnas.89.2.693.

15. Chen CM, Smith DM, Peters MA, et al. Production and design of more effective avian replication-incompetent retroviral vectors. *Dev Biol*. 1999;214(2):370-384. doi:10.1006/dbio.1999.9432.

16. HAMBURGER V, HAMILTON HL. A series of normal stages in the development of the chick embryo. *J Morphol*. 1951;88(1):49-92.

17. Kirby ML, Turnage KL, Hays BM. Characterization of conotruncal malformations following ablation of "cardiac" neural crest. *Anat Rec*. 1985;213(1):87-93. doi:10.1002/ar.1092130112.

18. Chai Y, Jiang X, Ito Y, et al. Fate of the mammalian cranial neural crest during tooth and mandibular morphogenesis. *Development*. 2000;127(8):1671-1679.

19. Lewis AE, Vasudevan HN, O'Neill AK, Soriano P, Bush JO. The widely used Wnt1-Cre transgene causes developmental phenotypes by ectopic activation of Wnt signaling. *Dev Biol*. 2013;379(2):229-234. doi:10.1016/j.ydbio.2013.04.026.

20. Tomita Y, Matsumura K, Wakamatsu Y, et al. Cardiac neural crest cells contribute to the dormant multipotent stem cell in the mammalian heart. *J Cell Biol*. 2005;170(7):1135-1146. doi:10.1083/jcb.200504061.

21. Tamura Y, Matsumura K, Sano M, et al. Neural crest-derived stem cells migrate and differentiate into cardiomyocytes after myocardial infarction. *Arterioscler Thromb Vasc Biol*. 2011;31(3):582-589. doi:10.1161/ATVBAHA.110.214726.

22. González-Rosa JM, Burns CE, Burns CG. Zebrafish heart regeneration: 15 years of discoveries. *Regeneration (Oxf)*. 2017;4(3):105-123. doi:10.1002/reg2.83.

23. Jopling C, Sleep E, Raya M, Martí M, Raya A, Izpisúa Belmonte JC. Zebrafish heart regeneration occurs by cardiomyocyte dedifferentiation and proliferation. *Nature*. 2010;464(7288):606-609. doi:10.1038/nature08899.

24. Carney TJ, Dutton KA, Greenhill E, et al. A direct role for Sox10 in specification of neural crest-derived sensory neurons. *Development*. 2006;133(23):4619-4630. doi:10.1242/dev.02668.

25. Abdul-Wajid S, Demarest BL, Yost HJ. Loss of embryonic neural crest derived cardiomyocytes causes adult onset hypertrophic cardiomyopathy in zebrafish. *Nat Commun*. 2018;9(1):4603. doi:10.1038/s41467-018-07054-8.

26. Tani-Matsuhana S, Vieceli FM, Gandhi S, Inoue K, Bronner ME. Transcriptome profiling of the cardiac neural crest reveals a critical role for MafB. *Dev Biol*. September 2018. doi:10.1016/j.ydbio.2018.09.015.

27. Martik ML, Bronner ME. Regulatory Logic Underlying Diversification of the Neural Crest. *Trends Genet*. 2017;33(10):715-727. doi:10.1016/j.tig.2017.07.015.

28. Lukoseviciute M, Gavriouchkina D, Williams RM, et al. From Pioneer to Repressor: Bimodal foxd3 Activity Dynamically Remodels Neural Crest Regulatory Landscape In Vivo. *Dev Cell*. 2018;47(5):608–628.e6. doi:10.1016/j.devcel.2018.11.009.

29. Sánchez-Iranzo H, Galardi-Castilla M, Minguillón C, et al. Tbx5a lineage tracing shows cardiomyocyte plasticity during zebrafish heart regeneration. *Nat Commun*. 2018;9(1):428. doi:10.1038/s41467-017-02650-6.

30. Schindler YL, Garske KM, Wang J, et al. Hand2 elevates cardiomyocyte production during zebrafish heart development and regeneration. *Development*. 2014;141(16):3112-3122. doi:10.1242/dev.106336.

31. Kikuchi K, Holdway JE, Werdich AA, et al. Primary contribution to zebrafish heart regeneration by gata4(+) cardiomyocytes. *Nature*. 2010;464(7288):601-605. doi:10.1038/nature08804.

32. Langmead B, Salzberg SL. Fast gapped-read alignment with Bowtie 2. *Nat Methods*. 2012;9(4):357-359. doi:10.1038/nmeth.1923.

33. Liao Y, Smyth GK, Shi W. featureCounts: an efficient general purpose program for assigning sequence reads to genomic features. *Bioinformatics*. 2014;30(7):923-930. doi:10.1093/bioinformatics/btt656.

34. Love MI, Huber W, Anders S. Moderated estimation of fold change and dispersion for RNA-seq data with DESeq2. *Genome Biol*. 2014;15(12):550. doi:10.1186/s13059-014-0550-8.

35. Mi H, Muruganujan A, Huang X, et al. Protocol Update for large-scale genome and gene function analysis with the PANTHER classification system (v.14.0). *Nat Protoc*. 2019;14(3):703-721. doi:10.1038/s41596-019-0128-8.

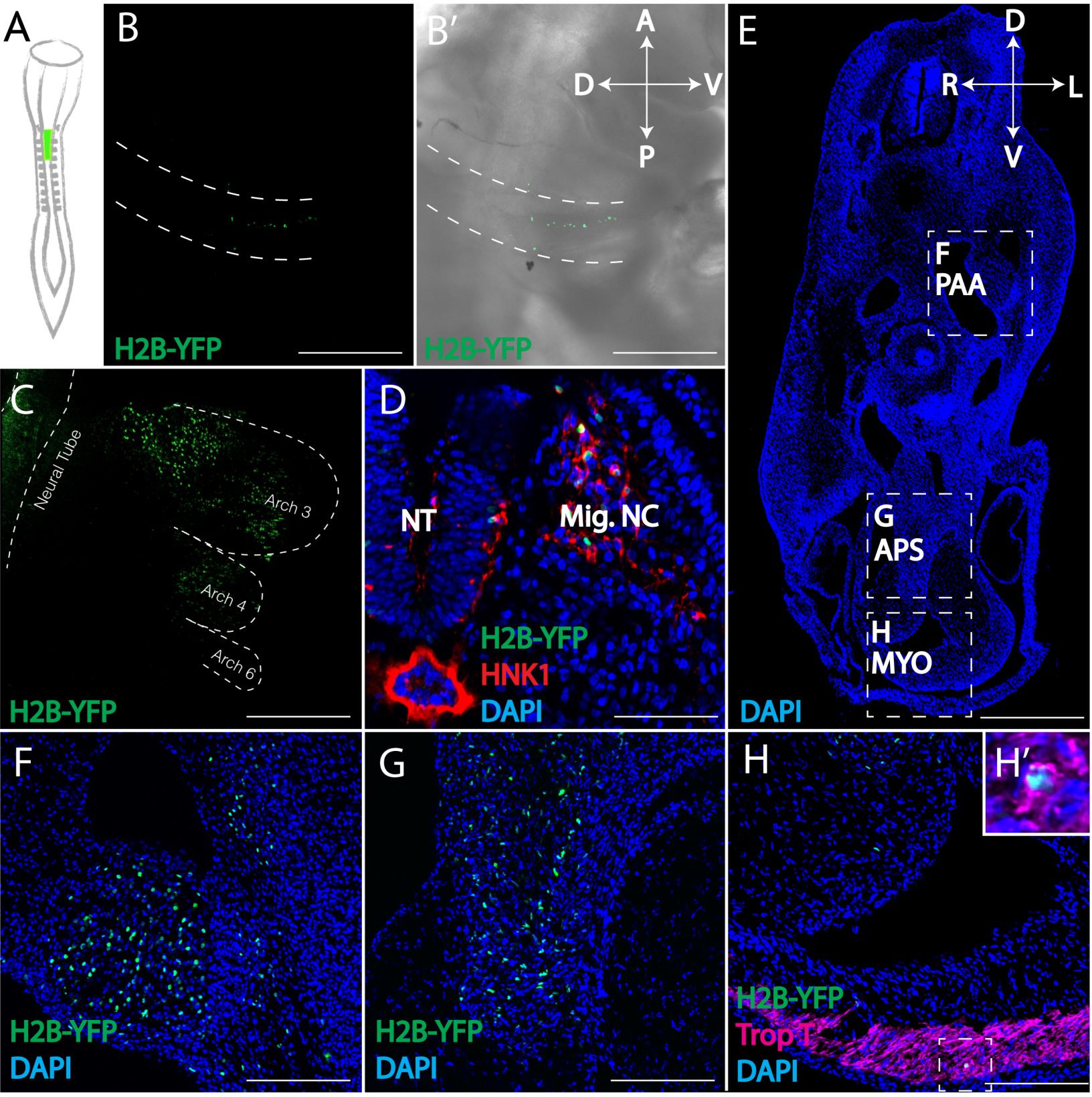

I

	MNC	CN-IX	PAA	APS	MYO	IVS
Day 1						
Day 2						
Day 3						
Day 4						
Day 5						
Day 6						
Day10						

Developmental time

Dorsal-ventral axis

Absent

Present (known)

Present (new)

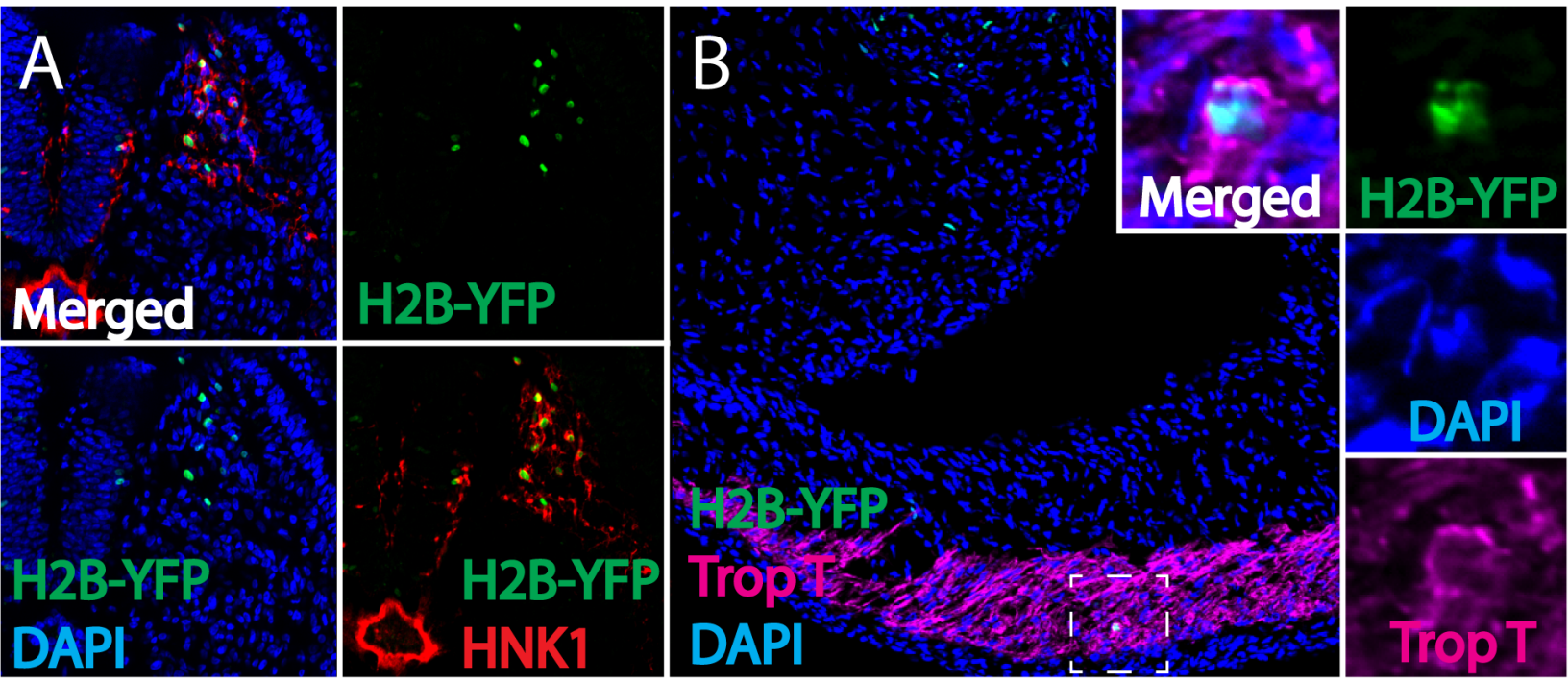
A
Merged
H2B-YFP
H2B-YFP
DAPI
H2B-YFP
HNK1
B
Merged
H2B-YFP
DAPI
H2B-YFP
Trop T
DAPI
Trop T

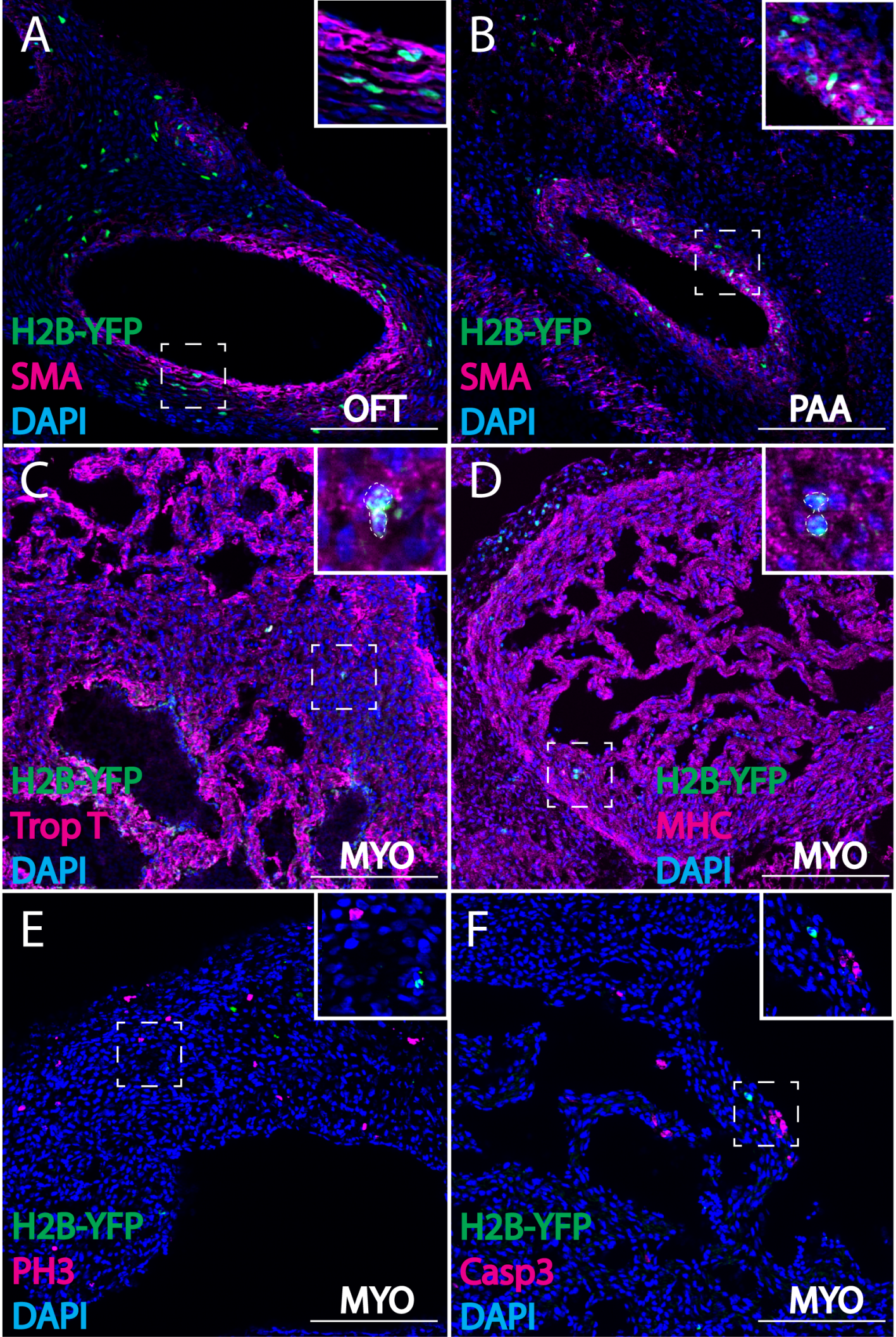
A
H2B-YFP
SMA
DAPI
OFT
B
H2B-YFP
SMA
DAPI
PAA
C
H2B-YFP
Trop T
DAPI
MYO
D
H2B-YFP
MHC
DAPI
MYO
E
H2B-YFP
PH3
DAPI
MYO
F
H2B-YFP
Casp3
DAPI
MYO

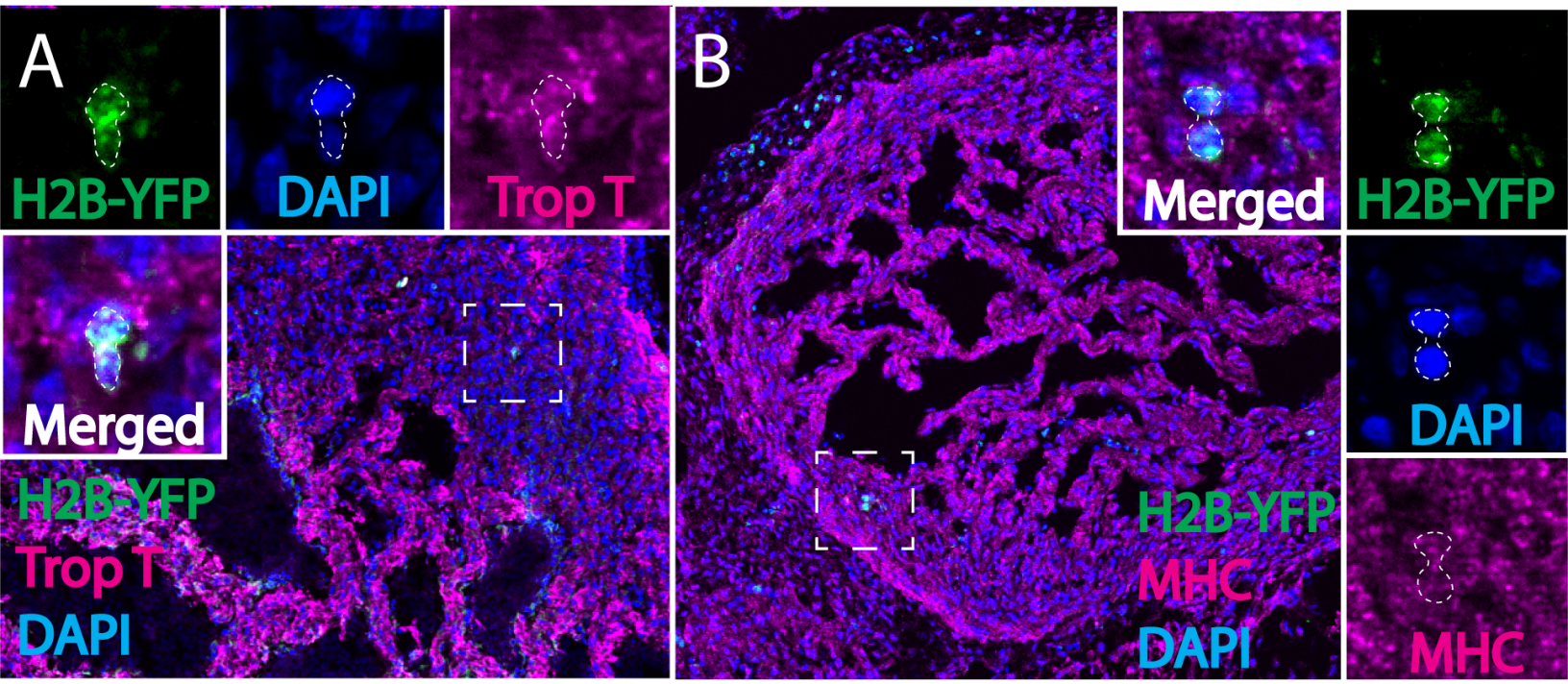
A
H2B-YFP
DAPI
Trop T
Merged
H2B-YFP
Trop T
DAPI
B
Merged
H2B-YFP
DAPI
H2B-YFP
MHC
DAPI
MHC

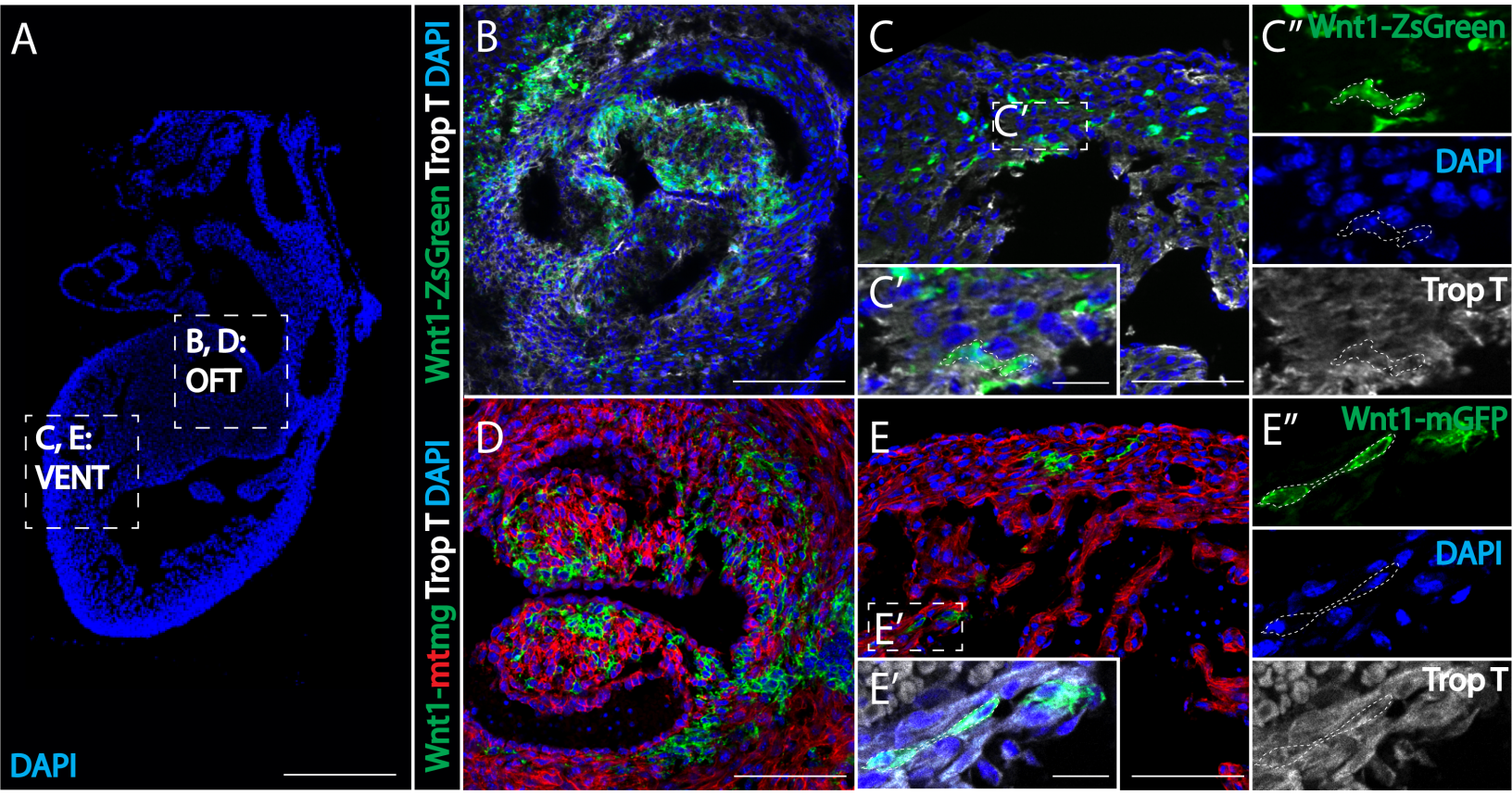
A
B, D:
OFT
C, E:
VENT
DAPI
Wnt1-ZsGreen Trop T DAPI
B
C
C′
C″ Wnt1-ZsGreen
DAPI
Trop T
Wnt1-mtmg Trop T DAPI
D
E
E′
E″ Wnt1-mGFP
DAPI
Trop T

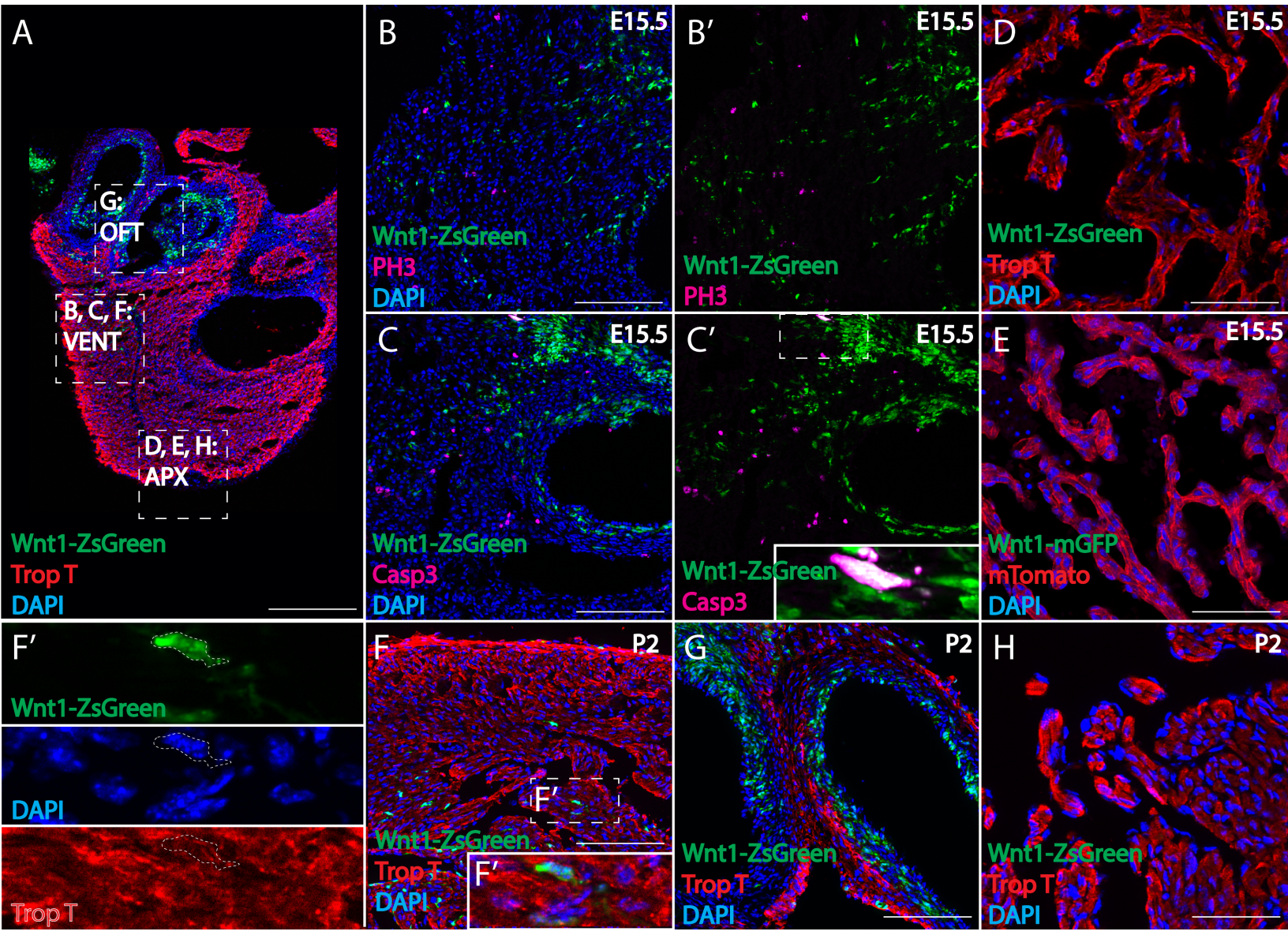
A
G:
OFT
B, C, F:
VENT
D, E, H:
APX
Wnt1-ZsGreen
Trop T
DAPI
B
E15.5
Wnt1-ZsGreen
PH3
DAPI
B′
E15.5
Wnt1-ZsGreen
PH3
D
E15.5
Wnt1-ZsGreen
Trop T
DAPI
C
E15.5
Wnt1-ZsGreen
Casp3
DAPI
C′
E15.5
Wnt1-ZsGreen
Casp3
E
E15.5
Wnt1-mGFP
mTomato
DAPI
F′
Wnt1-ZsGreen
DAPI
Trop T
F
P2
F′
Wnt1-ZsGreen
Trop T
DAPI
F′
G
P2
Wnt1-ZsGreen
Trop T
DAPI
H
P2
Wnt1-ZsGreen
Trop T
DAPI

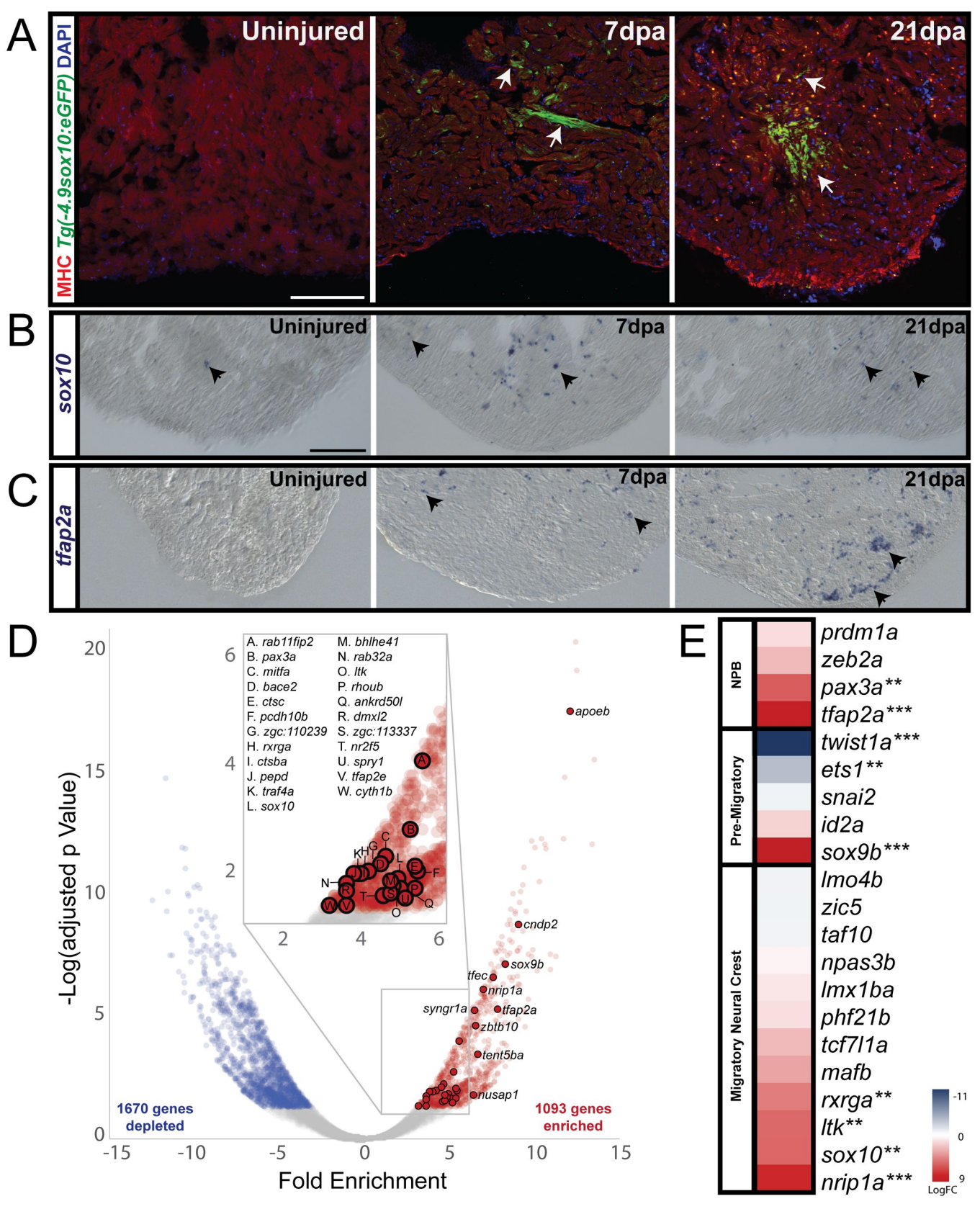
A
MHC Tg(-4.9sox10:eGFP) DAPI
Uninjured
7dpa
21dpa
B
sox10
Uninjured
7dpa
21dpa
C
tfap2a
Uninjured
7dpa
21dpa
D
-Log(adjusted p Value)
Fold Enrichment
1670 genes depleted
1093 genes enriched
A. rab11fip2
B. pax3a
C. mitfa
D. bace2
E. ctsc
F. pcdh10b
G. zgc:110239
H. rxrga
I. ctsba
J. pepd
K. traf4a
L. sox10
M. bhlhe41
N. rab32a
O. ltk
P. rhoub
Q. ankrd50l
R. dmxl2
S. zgc:113337
T. nr2f5
U. spry1
V. tfap2e
W. cyth1b
apoeb
cndp2
sox9b
tfec
nrip1a
syngr1a
tfap2a
zbtb10
tent5ba
nusap1
E
NPB
Pre-Migratory
Migratory Neural Crest
prdm1a
zeb2a
pax3a**
tfap2a***
twist1a***
ets1**
snai2
id2a
sox9b***
lmo4b
zic5
taf10
npas3b
lmx1ba
phf21b
tcf7l1a
mafb
rxrga**
ltk**
sox10**
nrip1a***
LogFC

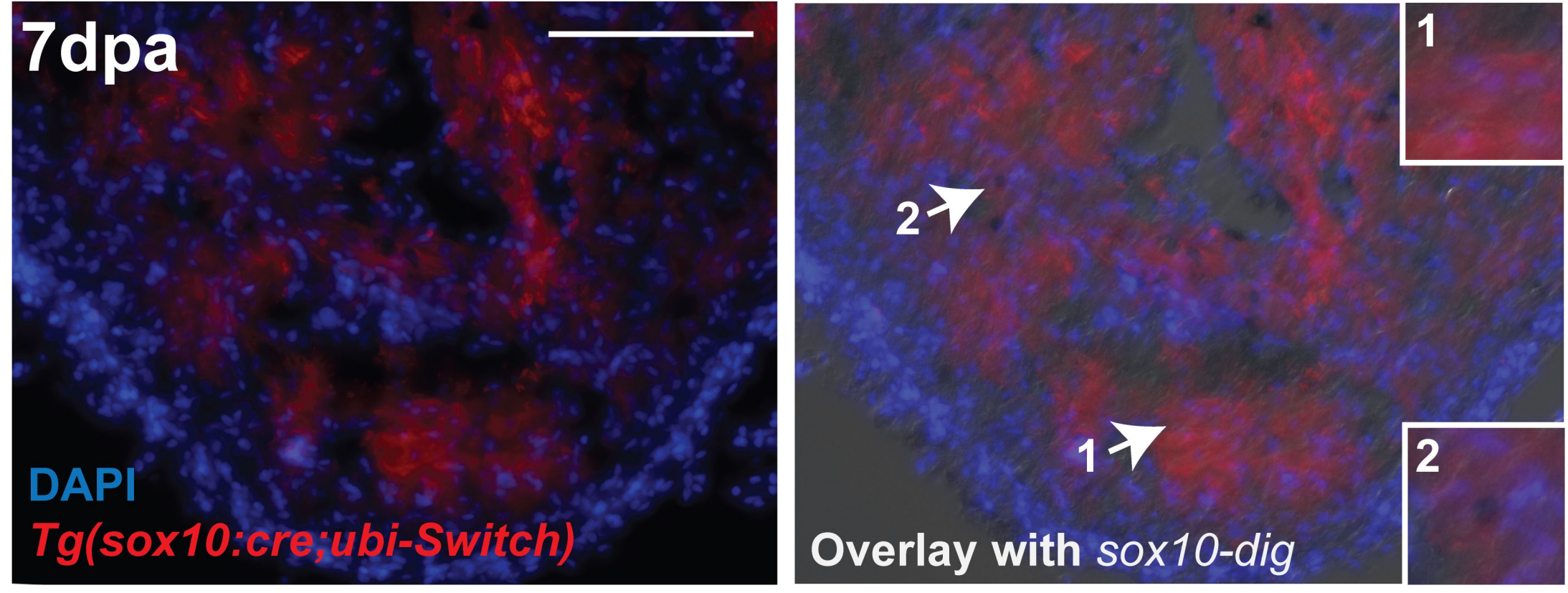
7dpa
DAPI
Tg(sox10:cre;ubi-Switch)
1
2
2
1
Overlay with sox10-dig

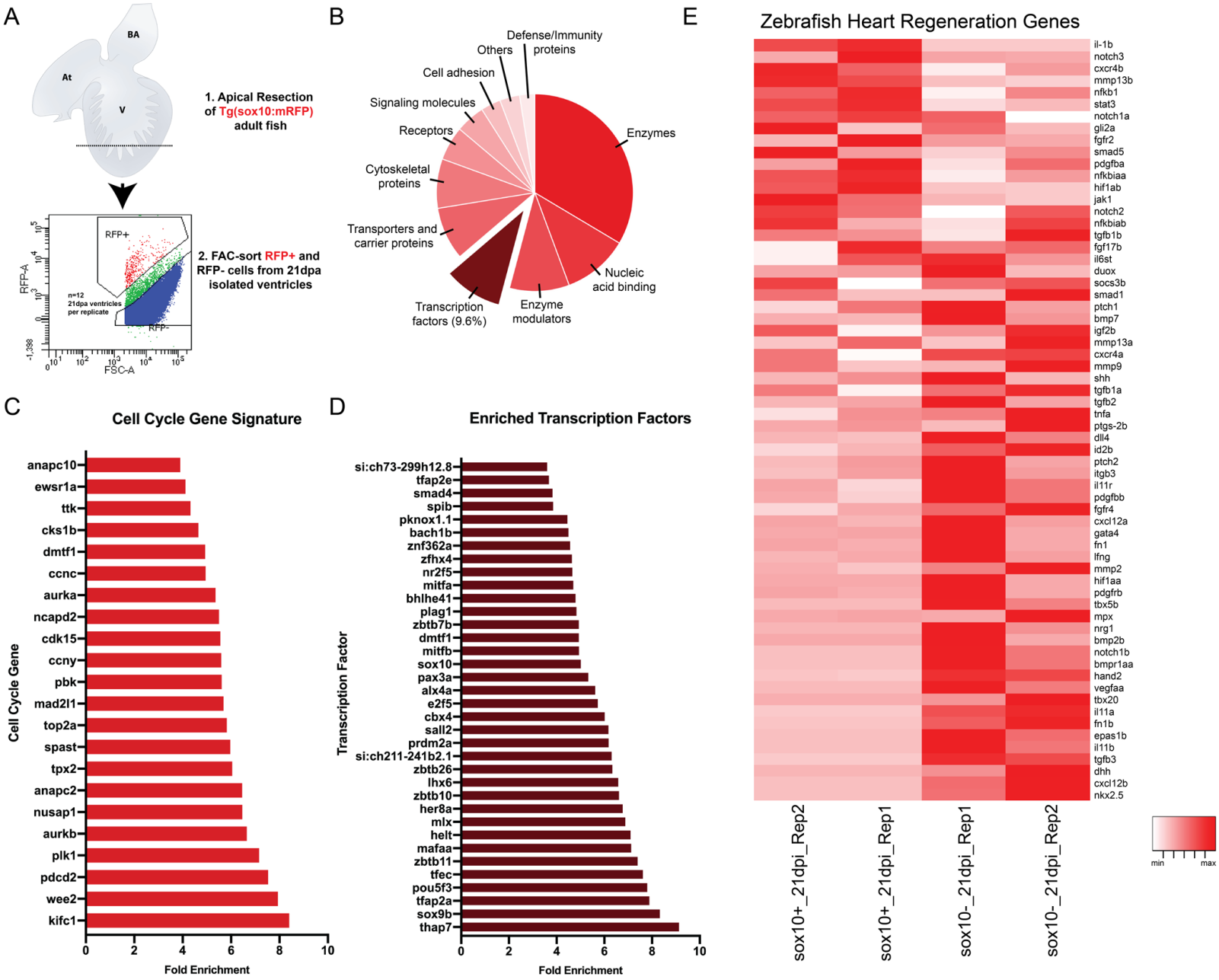
A
BA
At
V
1. Apical Resection of Tg(sox10:mRFP) adult fish
RFP+
RFP-
n=12 21dpa ventricles per replicate
RFP-A
FSC-A
2. FAC-sort RFP+ and RFP- cells from 21dpa isolated ventricles
B
Defense/Immunity proteins
Others
Cell adhesion
Signaling molecules
Receptors
Cytoskeletal proteins
Transporters and carrier proteins
Transcription factors (9.6%)
Enzyme modulators
Nucleic acid binding
Enzymes
C
Cell Cycle Gene Signature
Cell Cycle Gene
anapc10
ewsr1a
ttk
cks1b
dmtf1
ccnc
aurka
ncapd2
cdk15
ccny
pbk
mad2l1
top2a
spast
tpx2
anapc2
nusap1
aurkb
plk1
pdcd2
wee2
kifc1
Fold Enrichment
D
Enriched Transcription Factors
Transcription Factor
si:ch73-299h12.8
tfap2e
smad4
spib
pknox1.1
bach1b
znf362a
zfhx4
nr2f5
mitfa
bhlhe41
plag1
zbtb7b
dmtf1
mitfb
sox10
pax3a
alx4a
e2f5
cbx4
sall2
prdm2a
si:ch211-241b2.1
zbtb26
lhx6
zbtb10
her8a
mlx
helt
mafaa
zbtb11
tfec
pou5f3
tfap2a
sox9b
thap7
Fold Enrichment
E
Zebrafish Heart Regeneration Genes
il-1b
notch3
cxcr4b
mmp13b
nfkb1
stat3
notch1a
gli2a
fgfr2
smad5
pdgfba
nfkbiaa
hif1ab
jak1
notch2
nfkbiab
tgfb1b
fgf17b
il6st
duox
socs3b
smad1
ptch1
bmp7
igf2b
mmp13a
cxcr4a
mmp9
shh
tgfb1a
tgfb2
tnfa
ptgs-2b
dll4
id2b
ptch2
itgb3
il11r
pdgfbb
fgfr4
cxcl12a
gata4
fn1
lfng
mmp2
hif1aa
pdgfrb
tbx5b
mpx
nrg1
bmp2b
notch1b
bmpr1aa
hand2
vegfaa
tbx20
il11a
fn1b
epas1b
il11b
tgfb3
dhh
cxcl12b
nkx2.5
sox10+_21dpi_Rep2
sox10+_21dpi_Rep1
sox10-_21dpi_Rep1
sox10-_21dpi_Rep2
min
max